Journal of
Analytical & Bioanalytical Techniques

Konishi et al., J Anal Bioanal Tech 2017, 8:5
DOI: 10.4172/2155-9872.1000378

Research Article OMICS International

Potentiometric and ^{1}H NMR Spectroscopic Studies of Functional Monomer Influence on Histamine-Imprinted Polymer-Modified Potentiometric Sensor Performance

Atsuko Konishi*, Shigehiko Takegami, Shoko Akatani, Rie Takemoto and Tatsuya Kitade

Department of Analytical Chemistry, Kyoto Pharmaceutical University, 5 Nakauchicho, Misasagi, Yamashina-ku, Kyoto 607-8414, Japan

Abstract

For the development of a histamine (HIS) potentiometric sensor based on molecularly imprinted polymers (MIPs), the effects of four functional monomers, namely acrylamide (AA), atropic acid (AT), methacrylic acid (MAA), and 4-vinylpyridine (4-VP), from which the MIP was synthesized, on the performance of the HIS sensor were examined by potentiometric and ^{1}H nuclear magnetic resonance (NMR) spectroscopic methods. The intermolecular interactions between HIS as a template molecule and a functional monomer were investigated based on the ^{1}H NMR spectra of HIS in distilled water in the presence of each functional monomer. Changes to the chemical shift of each HIS proton indicated that HIS typically formed a HIS-functional monomer complex at a ratio of 1:1 via hydrogen bonding with AA, AT and MAA, and interacted with 4-VP between the imidazole ring and pyridine ring of 4-VP. The potential changes of the four HIS sensors were measured in 0.1×10^{-3} mol L^{-1} aqueous solution using Ag/AgCl as a reference electrode; the order of the magnitudes of the changes was MAA>AA=4-VP>AT. The potential changes of three non-imprinted polymer-modified potentiometric sensors prepared without HIS were smaller than those of the corresponding HIS sensors, except in the case of AT. The potential response and selectivity of the HIS sensor using MAA were better than those of the other three HIS sensors. The ^{1}H NMR spectroscopic and potentiometric results showed that the hydrogen bond between HIS and MAA strongly and effectively influenced the potential response of the HIS sensor.

Keywords: Potentiometric sensor; Molecularly imprinted polymer; Intermolecular interaction; ^{1}H NMR spectroscopy; Histamine; Functional monomer

Introduction

Chemical sensors consist of a recognition element and a transducer. The recognition element recognizes only the analyte, and the transducer converts the recognized information to electrical signals. In the development of chemical sensors, the recognition element is therefore the important factor in detecting an analyte specifically and selectively. Biosensors using biological materials as the recognition element have been developed because enzyme–substrate [1,2] and antigen–antibody [3] reactions are highly specific. Biosensors are widely used in clinical applications such as self-monitoring blood glucose meters [4]. However, there are problems in using biological materials; e.g., they are unstable and expensive.

A molecularly imprinted polymer (MIP) is an artificial tailor-made receptor capable of selectively recognizing and binding target molecules with high affinity. As shown in Figure 1, an MIP is a highly cross-linked polymer. The process usually involves initiating polymerization of a cross-linker with a functional monomer in the presence of a template molecule, which is subsequently extracted, leaving complementary cavities behind [5,6]. The MIP provides binding sites that are complementary in size, shape, and functionality to the template molecule; therefore, the template molecule preferentially rebinds to the cavity. MIPs have many advantages: they are tailor-made, stable, and inexpensive. Recently, MIPs have been studied for many applications such as high-performance liquid chromatography column packings [5,6], solid-phase extraction [7-9], drug-delivery systems [10-13], and sensors [14,15]. Chemical sensors based on MIPs can overcome some of the problems of biosensors.

Histamine (HIS), which is shown in Figure 2A, is important in inflammation, immediate allergic reactions [16], and gastric acid secretion, and acts as a neurotransmitter in the brain [17]. Also, HIS in fish causes allergy-like food poisoning in humans [18]. Because the determination of HIS in blood, urine, and food is therefore important, method developments in this field have been reported, e.g., amperometric determination [19-21] and fluorescent determination using ribonucleopeptide [22]. However, many of the methods employ biosensors.

For the development of MIP-modified potentiometric HIS sensors with good responsivity and selectivity, it is important to investigate the intermolecular interactions between HIS and functional monomers. In this study, we used four functional monomers, i.e., acrylamide (AA), atropic acid (AT) and methacrylic acid (MAA), and 4-vinylpyridine (4-VP), which are neutral, acidic, and basic functional monomers, respectively (Figure 2B-2E). The aims of this study were to elucidate the intermolecular interactions between HIS and each functional monomer and to clarify how each functional monomer affects the responsivity and selectivity of the HIS sensor. First, the intermolecular interactions between HIS and each functional monomer were investigated based on the chemical shift changes of each HIS proton in the presence of

***Corresponding author:** Atsuko Konishi, Department of Analytical Chemistry, Kyoto Pharmaceutical University, 5 Nakauchicho, Misasagi, Yamashina-ku, Kyoto 607-8414, Japan, Tel: +81755954659; Fax: +81755954760; E-mail: konishi@mb.kyoto-phu.ac.jp

Received August 21, 2017; **Accepted** October 05, 2017; **Published** October 12, 2017

Citation: Konishi A, Takegami S, Akatani S, Takemoto R, Kitade T (2017) Potentiometric and ^{1}H NMR Spectroscopic Studies of Functional Monomer Influence on Histamine-Imprinted Polymer-Modified Potentiometric Sensor Performance. J Anal Bioanal Tech 8: 378. doi: 10.4172/2155-9872.1000378

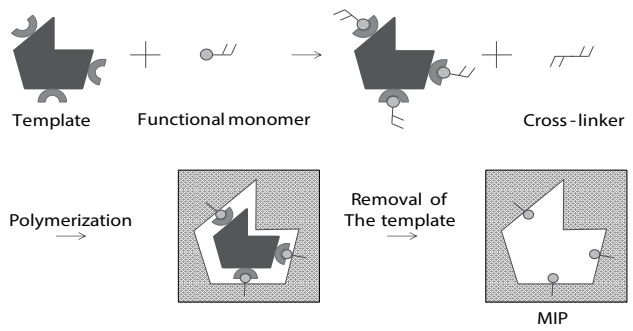

Figure 1: Schematic diagram of preparation of molecularly imprinted polymer (MIP).

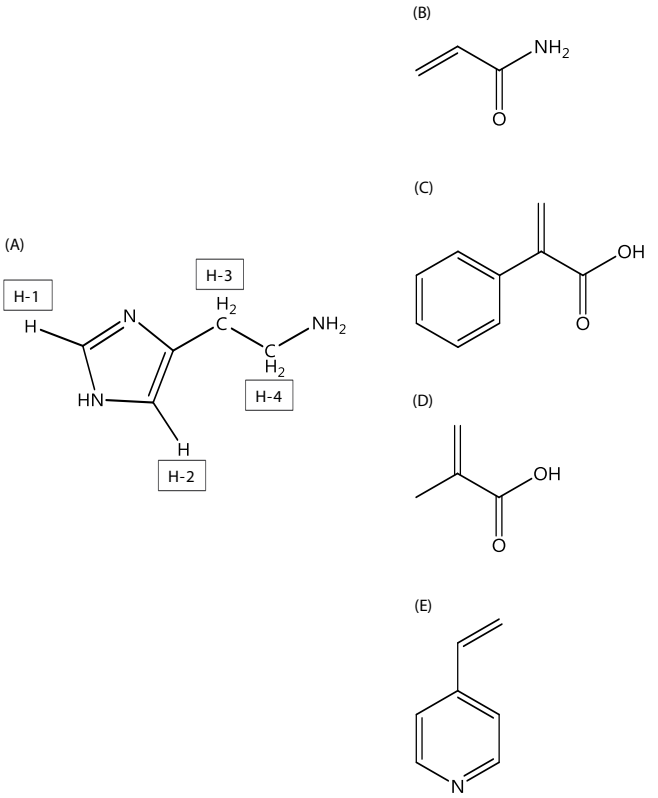

Figure 2: Chemical structures of (A) template molecule, i.e., HIS (log *P*-0.70), and functional monomers (B) AA, (C) AT, (D) MAA, and (E) 4-VP.

each functional monomer using ^{1}H nuclear magnetic resonance (NMR) spectroscopy. Next, the responsivities and selectivities of four HIS sensors containing the functional monomers were assessed by measuring the potential changes in the presence of HIS and other chemical substances. The effects of the intermolecular interactions between HIS and the functional monomer on the performance of the HIS sensor were examined.

Experimental

Materials

Graphite rods were purchased from Strem Chemicals Inc. (Newburyport, MA, USA). Ethylbenzene was purchased from the Kanto Chemical Co., Inc. (Tokyo, Japan). 2-Aminobenzimidazole and deuterium oxide (99.9%) were purchased from Sigma-Aldrich (St. Louis, MO, USA). HIS dihydrochloride and AT were purchased from the Tokyo Chemical Industry Co., Ltd. (Tokyo, Japan). Sodium dodecyl sulfate (SDS), 2,2'-azobis(2,4-dimethylvaleronitrile) (V-65), dibutyl phthalate, AA, MAA, 4-VP, ethylene dimethacrylate (EDMA), poly(vinyl alcohol) (PVA) 1000 (partially hydrolyzed PVA), methanol, pyrrole, histidine, and L(+)-lysine hydrochloride were purchased from Wako Pure Chemical Industries, Ltd. (Kyoto, Japan). The hydroquinone added to EDMA as a stabilizer was extracted with NaOH before use. Toluene was purchased from Nacalai Tesque, Inc. (Kyoto, Japan).

^{1}H NMR spectra

Aliquots of an HIS stock solution were placed in 2-mL volumetric flasks. A desired amount of a functional monomer stock solution, i.e., AA, AT, MAA, or 4-VP, was added, and distilled water was added to volume. The final concentrations of HIS and each functional monomer were 1.0×10^{-3} mol L^{-1}, and 0.0, 1.0×10^{-3}, 2.0×10^{-3}, 3.0×10^{-3} mol L^{-1} for AA, MAA and 4-VP, and 0.0, 1.0×10^{-3}, 2.0×10^{-3} mol L^{-1} for AT (because of low water solubility), respectively. The flasks were shaken for a short time and then samples were transferred to NMR tubes of diameter 5 mm. A coaxial internal tube containing ca. 2.0×10^{-2} mol L^{-1} 3-(trimethylsilyl)propionic-2,2,3,3-d_4 acid sodium salt (98 atom% D) in D_2O was inserted into the sample tube to provide a reference signal. ^{1}H NMR spectra were recorded with a Unity Inova 400NB spectrometer (Agilent Technologies, Inc., CA, USA) operated at 399.97 MHz, using a presaturation method to reduce the signal of protons derived from H_2O. The probe temperature was 25 ± 1°C. An accumulation of 200 free induction decays was used to improve the signal-to-noise ratio.

Sensor synthesis

The HIS sensor was prepared using a modified version of a previously reported procedure [23]. A graphite rod (diameter 3 mm, length 50 mm) was used as a transducer. The graphite rod was polished with sandpaper and then sonicated five times for 5 min in distilled water. A plasma polymerized thin film of ethylbenzene was deposited on the surface of the polished graphite rod using a plasma deposition system (BP-1, Samco Inc., Kyoto, Japan). The first swelling step was performed by immersing the plasma-coated graphite in a suspension of SDS (0.55 mmol) as a surfactant, V-65 (1.37 mmol) as a radical initiator, dibutyl phthalate (14.3 mmol) as a plasticizer, and distilled water (40 mL). The mixture was stirred at room temperature for 24 h. In the second swelling step, the graphite was immersed in PVA solution (10.67 g/500 mL) containing HIS (2 mmol) as a template molecule, a functional monomer (20 mmol), EDMA (25 mmol) as a cross-linker, and toluene (47 mmol) as a porogen. The mixture was stirred at room temperature for 24 h, and then degassed using helium and polymerized by heating at 70-75°C for 12 h. The graphite was then immersed in methanol to remove the HIS. This procedure was repeated until the ultraviolet absorption of HIS in methanol at 210 nm was not observed. The HIS sensor was stored in distilled water. Non-imprinted (NIP) sensors were prepared using the same procedure, but without HIS.

Sensor measurements

The HIS sensor and an Ag/AgCl reference electrode were immersed in distilled water (100 mL) and the potential response of the HIS sensor against the reference electrode was measured by a potentiometer (pH meter F-52, Horiba Inc., Kyoto, Japan). When the potential response was stable, record was started. After 1 min from the start, 1.0×10^{-2} mol L^{-1} stock solution (1 mL) of each chemical substance was injected into

the distilled water. The potential response value at the start of record was set to 0 mV and potential change was defined as the difference between the potential response values before and after the addition of each chemical substance. The sensor selectivity was tested by comparing the responses of the template molecule HIS and other chemicals with similar chemical structures or *n*-octanol/water partition coefficients (log *P*), namely histidine, 2-aminobenzimidazole, pyrrole, and lysine.

Results and Discussion

^{1}H NMR study of intermolecular interactions between HIS and functional monomers

^{1}H NMR spectra of HIS mixed with each functional monomer, i.e., AA, AT, MAA, and 4-VP, in H_2O were recorded to determine which functional monomer had the highest affinity with HIS. ^{1}H NMR spectra of HIS-functional monomer systems having a ratio of 1:1 are shown in Figure 3 as an example. The HIS (see structure in Figure 2A) proton signals were observed at 8.61 (H-1), 7.37 (H-2), 3.15 (H-3), and 3.35 (H-4) ppm (Figure 3A). Figure 3B-3D shows that the addition of AA, AT, and MAA shifts the HIS proton signals to slightly lower fields. In contrast, in the presence of 4-VP (Figure 3E), the H-1, H-2 and H-3 signals shifted to higher fields, with the H-4 signal showing almost no change.

The chemical shifts of the HIS protons were measured in the absence and presence of each functional monomer; the results for HIS H1–H4 are shown in Figure 4A-4D. As shown in Figure 4A and 4B, the HIS H-1 and H-2 signals were shifted to lower fields in the presence of AT and MAA at concentrations of 1.0×10^{-3} mol L^{-1}. In the presence of AA, small downfield shifts of the HIS H-1 and H-2 signals were also observed, however, the shifts were smaller than those in the presence of AT and MAA. Further increasing the concentration of the monomer above 1.0×10^{-3} mol L^{-1} resulted in no significant change to the chemical shift values. Additionally, Figure 4C-4D shows that regardless of the monomer concentration for AA, AT, and MAA, no significant change to the chemical shift values of the HIS H-3 and H-4 signals were observed. These results indicate that HIS can form a complex with the aforementioned functional monomers at a ratio of 1:1 and the imidazole ring of HIS interacts with the functional monomer. The acid dissociation constants (pK_as) of HIS are 6.15 and 9.84 for the nitrogen atom of the secondary amine on the imidazole ring and the primary amino group on the side chain, respectively [24,25]. The pK_a values of AT [26], MAA [27], and 4-VP [26] are 4.0, 4.66, and 6.0, respectively. The pK_a of AA is above 15 and the proton of the amide does not dissociate under normal conditions. Since the ionization states of HIS and functional monomers depend on the pH value of the sample solution, the pH values of the HIS solution and the mixtures of HIS and each functional monomer used in the ^{1}H NMR experiments were therefore measured. These results were 4.7 ± 0.0 for HIS (*n*=3), 4.6 ± 0.1 for HIS/AA, 3.3 ± 0.1 for HIS/AT, 3.7 ± 0.2 for HIS/MAA and 6.0 ± 0.2 for HIS/4-VP (*n*=3 at each functional monomer concentration). Under the experimental conditions in the presence of AA, AT or MAA, the di-cationic form of HIS is protonated at the primary amino group on the side chain and the nitrogen atom of the secondary amine on the imidazole ring. Conversely, AA, AT and MAA are neutral. Previous ^{1}H NMR investigations have reported that the proton chemical shift is shifted to lower fields by the formation of a hydrogen bond between the template and the functional monomer, and the larger the chemical shift, the stronger the interaction between them [28,29]. Additionally, it has previously been reported that the di-cationic form of HIS forms a complex with MAA more easily than the mono-cationic form in aqueous media [30,31]. Therefore, since the change in chemical shift for the HIS H-1 signal was larger than the corresponding H-2 shift in the presence of AA, AT and MAA, HIS may complex with the functional monomers at a ratio of 1:1 as shown in Figure 4E - an example illustration of the HIS-MAA complex. Furthermore, the strength of the hydrogen bond to form the HIS-functional monomer complex was in the order of HIS-AT>HIS-MAA>HIS-AA.

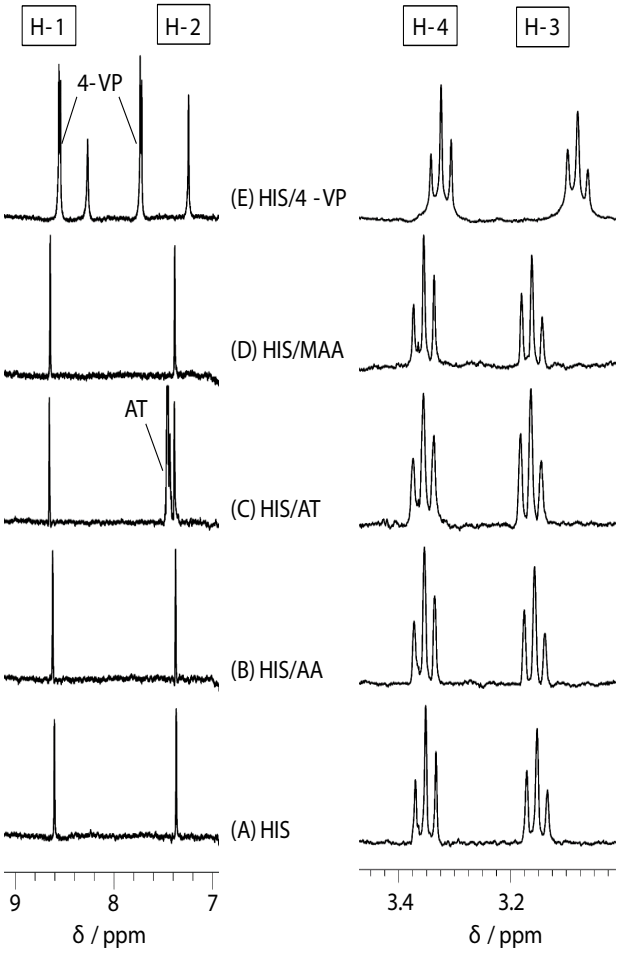

Figure 3: ^{1}H NMR spectra of (A) 1.0×10^{-3} mol L^{-1} HIS alone, and mixtures of 1.0×10^{-3} mol L^{-1} HIS and functional monomer, (B) AA, (C) AT, (D) MAA, and (E) 4-VP, in distilled water. The 3-(trimethylsilyl)propionic-2,2,3,3-d_4 acid sodium salt (98 atom% D) signal was set to 0 ppm as an internal reference.

In contrast, in the presence of 4-VP, all HIS H1–H4 signals shifted to higher fields depending on the 4-VP concentration. Under the experimental conditions in the presence of 4-VP, i.e., pH 6.0, HIS is present in equal quantities of mono-cationic and di-cationic forms with the former protonated only at the primary amino group on the side chain. Meanwhile, 4-VP is 50% neutral and 50% as a mono-cationic species, which is protonated at the nitrogen atom of the tertiary amine on the pyridine ring. The large upfield shifts of the HIS H-1 and H-2 signals in the presence of 4-VP is thought to be the result of the proton exchange between the tertiary and secondary amine on the imidazole ring of HIS and the tertiary amine on the pyridine ring of 4-VP. It has been previously reported that the electrostatic interactions between the protonated amino group and the π-electron-

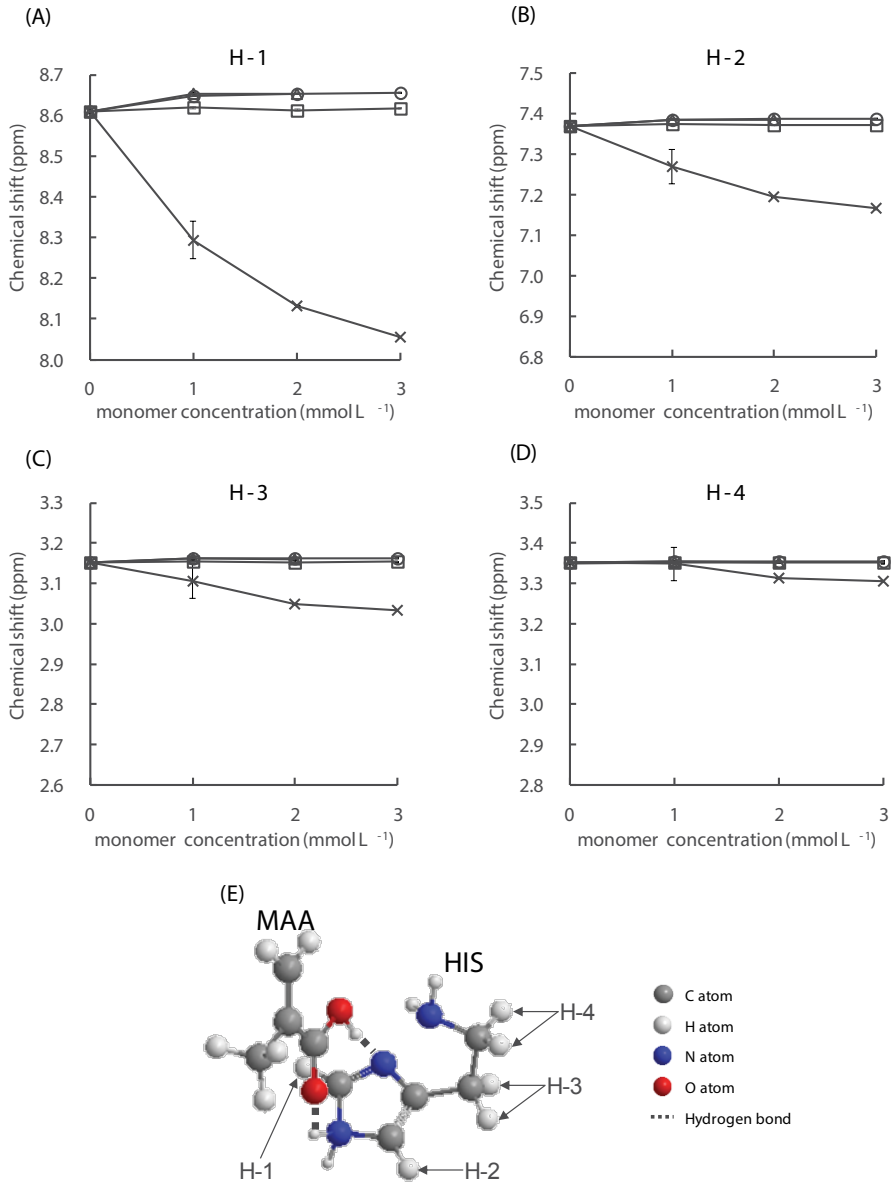

Figure 4: Chemical shift of each HIS proton, (A) H-1, (B) H-2, (C) H-3, and (D) H-4, in the absence and presence of the functional monomers as a function of concentration. (□) AA, (Δ) AT, (○) MAA, and (×) 4-VP. (E) Three-dimensional structure of the hydrogen bond between HIS and MAA.

rich pyridine ring can result in chemical shift changes to higher fields [32-34]. If the protonated amino group on the HIS side chain interacts with the pyridine ring of 4-VP, the HIS H-4 shift to higher fields will be greater than the H-3 shift. However, since changes to the chemical shift was in the order of H-1>H-2>H-3>H-4, the results indicate that HIS can interact with 4-VP between the HIS imidazole ring and the pyridine ring of 4-VP, but not between the protonated amino group on the HIS side chain and the pyridine ring of 4-VP. Unfortunately, the results of the ^{1}H NMR investigations could not yield details on how HIS complexes with 4-VP. The results of this ^{1}H NMR study partly clarify the intermolecular interactions between HIS and the functional monomers in bulk water and show that the order of magnitude of the interactions is: 4-VP>AT>MAA>AA.

Responsivities of four HIS sensors

The potential response values of four HIS sensors and NIP sensors prepared using each functional monomer on addition of 1.0×10^{-2} mol L^{-1} HIS stock solution was recorded; the curves are shown in Figure 5. The potential response value of each HIS sensor increased immediately after addition of HIS stock solution, reached a plateau after 15 s, and then showed a stable potential until 25 min. Potential changes of each HIS sensor at 1500 s after addition of HIS stock solution were shown in Figure 6. As shown in Figure 6, the order of the potential change magnitudes tended to be MAA>AA=4-VP>AT; i.e., the HIS sensor containing MAA showed the largest potential change among the four HIS sensors. These results and those of the ^{1}H NMR spectroscopic

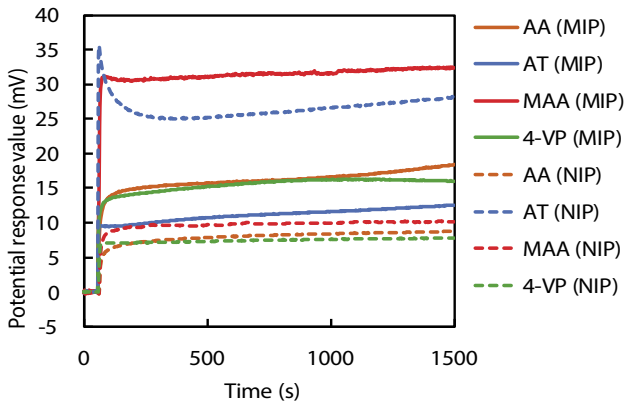

Figure 5: Potential response curves of HIS sensors and non-imprinted (NIP) sensors containing different functional monomers after addition of HIS aqueous solution. Final HIS concentration was 0.1 × 10^{-3} mol L^{-1}.

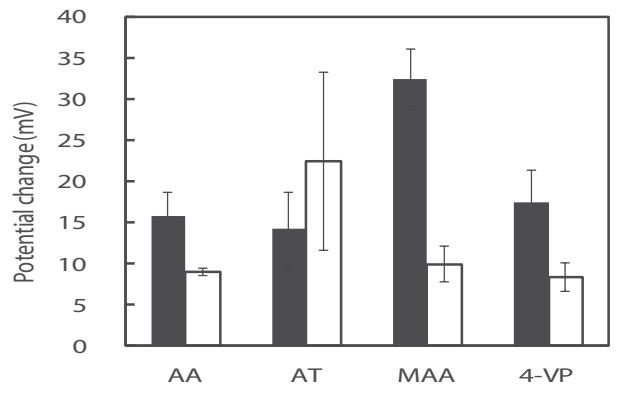

Figure 6: Potential changes of (■) HIS sensors and (□) corresponding NIP sensors at 1500 s after addition of HIS aqueous solution. The determination of HIS sensor and NIP sensor using each functional monomer was in triplicate, respectively.

study show that the relationship between the potential responses of the HIS sensors and the interactions between HIS and each functional monomer can be described as follows. The hydrogen bond between HIS and MAA plays an important role in the potential response of the HIS sensor. However, the potential change of the HIS sensor using AT as the functional monomer was smaller than the others, although the ^{1}H NMR spectroscopic results show that HIS also formed a complex with AT via hydrogen bond. This is considered to be the result of steric hindrance by the AT benzene ring, which is oriented towards the template cavity of the MIP. As the AT benzene ring occupies the cavity void, HIS ingress into the template cavity is hindered because of the aforementioned steric hindrance. As a result, HIS, especially the tertiary and protonated secondary amine on the imidazole ring, cannot bind to the carboxyl group of AT in the template cavity. The ^{1}H NMR spectra also show that HIS has the strongest and weakest interactions with 4-VP and AA, respectively; the potential changes of the HIS sensors using these monomers were almost the same. Although there are strong interactions between HIS and 4-VP, these interactions did not greatly affect the potential changes of the HIS sensors. The HIS di-cationic form interacts with AA via weak hydrogen bond, but the HIS sensor using AA responded to these hydrogen bonds and showed the same potential response as that of the HIS sensor using 4-VP. Our HIS sensor therefore mainly responds to surface potential changes caused by hydrogen-bond formation between the template molecule and the functional monomer.

Figure 6 also shows the potential changes for NIP sensors using each functional monomer at 1500 s after addition of HIS stock solution. The potential changes of the NIP sensors using AA, MAA, and 4-VP were significantly smaller than those of the corresponding HIS sensors; however, the potential change of the NIP sensor using AT was larger than that of the corresponding HIS sensor. Usually, the potential change of an NIP sensor is smaller than that of the corresponding HIS sensor because the NIP sensor does not have a HIS template, which provides highly specific HIS-binding sites. The NIP sensors should show no potential response to HIS, but small potential changes were observed for AA, MAA, and 4-VP. This is considered to be the result of non-specific binding and adsorption of HIS on the NIP sensor surface. Both MIP and NIP are hydrophobic polymers prepared using EDMA as a cross-linker. Additionally, the larger numbers of functional groups of each functional monomer may be exposed from the NIP surface when compared with the MIP surface, because the majority of the functional monomers used in the MIP preparations are involved in the construction of the template cavity. Although the di-cationic form of HIS non-specifically binds to the functional group, or adsorbs onto the hydrophobic MIP and NIP surface, the contribution of non-specific binding and hydrophobic adsorption will be larger on NIP than MIP. As a result, the NIP sensor showed a small potential change in response to the non-specific binding and adsorption of HIS on its surface. The surface of the NIP sensor using AT was more hydrophobic than those of the other NIP sensors because AT has a benzene ring in its molecular structure. The increase in non-specific adsorption of HIS on the hydrophobic surface, in addition to the hydrogen bonds between di-cationic HIS and AT, leads to a larger potential change for the NIP sensor using AT than for the other NIP sensors.

The specificities of HIS sensors using each functional monomer were easily compared by calculating the ratio of the potential change of each HIS sensor to that of the corresponding NIP sensor and their ratios were 1.8, 0.6, 3.3, and 2.1 for AA, AT, MAA, and 4-VP, respectively. Therefore, the specificity of the HIS sensor using MAA was also higher than those of the other HIS sensors.

The potentiometric results show that the HIS sensor using MAA gave the best response of the four HIS sensors because of the specific recognition of HIS based on hydrogen bonds between HIS and the carboxylic group of MAA in the MIP template cavity.

Selectivities of HIS sensors

The selectivities of the HIS sensors using different functional monomers were investigated by comparing their responses to four other chemicals, i.e., histidine, 2-aminobenzimidazole, pyrrole, and lysine (the structures are shown in Figure 7), with their responses to HIS. Histidine is very similar in chemical structure to HIS and has a carboxyl group. The log *P* values are -0.70, -3.56, 0.91, 0.75 and -3.05 for HIS, histidine, 2-aminobenzimidazole, pyrrole, and lysine respectively [35-38]. Figure 8 shows the potential change curves of the HIS sensor using MAA after addition of each chemical as an example. The potential response curve of HIS differed significantly from those of the other chemicals. For HIS, the HIS sensor showed a potential response value with a large gradient immediately after the addition of HIS stock solution. For the other four chemicals, there was no response or the potential response values gradually decreased with time. These results indicate that this sensor specifically recognized HIS but responded

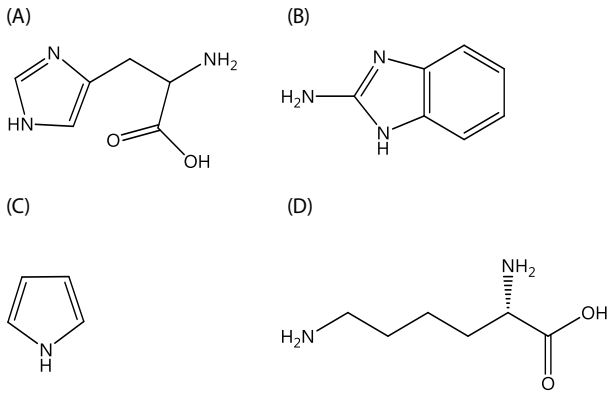

Figure 7: Chemical structures of (A) histidine, (B) 2-aminobenzimidazole, (C) pyrrole, and (D) lysine.

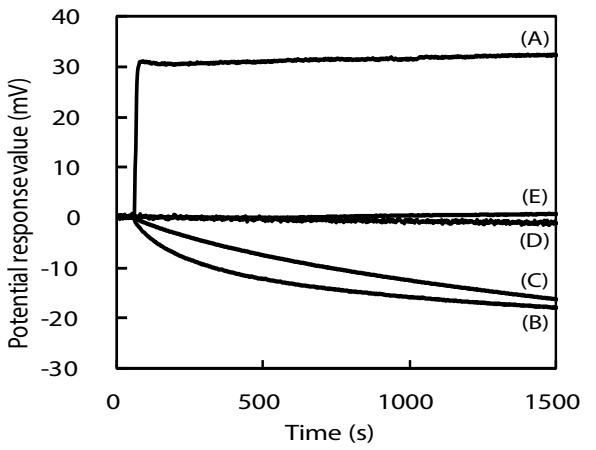

Figure 8: Potential response curves of HIS sensor using MAA to (A) HIS, (B) histidine, (C) 2-aminobenzimidazole, (D) pyrrole, and (E) lysine. Final concentration of chemical substances was 0.1×10^{-3} mol L^{-1}.

non-specifically to other chemicals adsorbed on the MIP surface of the HIS sensor. The same results were obtained for the other HIS sensors using AA, AT, and 4-VP.

Figure 9 shows the potential changes of the four HIS sensors in the presence of each chemical substance. Three HIS sensors, i.e., those using AA, AT, and 4-VP, showed large potential changes in response to 2-aminobenzimidazole. This large potential change was derived from adsorption of 2-aminobenzimidazole on the hydrophobic surface of MIP because of the large log *P* value of 2-aminobenzimidazole. In contrast, the HIS sensor using MAA showed a larger potential change to HIS than to the other four chemical substances, because MIP template cavity formed complementary to HIS and hydrogen bonds between HIS and MAA acted effectively to catch HIS in the sample solutions. As a result, the HIS sensor using MAA gave better selectivities than the three HIS sensors using AA, AT, and 4-VP.

To prove that the responsivity and selectivity of the HIS sensor using MAA were as a result of MIP specifically recognizing HIS, the potential change of the bare graphite rod electrode and the graphite rod electrode coated with the polymerized thin film of ethylbenzene were recorded as a function of sequential addition of each chemical substance (Figure 10). The bare graphite rod electrode responded to all chemical substances the same as the HIS sensor, however, the electrode shows a greater potential response for histidine, 2-aminobenzimidazole and pyrrole, and a smaller potential response for HIS when compared with the HIS sensor. No potential response was observed for lysine. Meanwhile, the graphite rod electrode coated with the polymerized thin film of ethylbenzene shows smaller potential response than the bare graphite rod electrode across all the chemical substances. However, comparing the HIS sensor using MAA (Figure 8) with the bare graphite rod electrode and the graphite rod electrode coated with the polymerized thin film of ethylbenzene, the potential response of the HIS sensor using MAA is significantly larger toward HIS and smaller to other chemical substances than that observed for both of the electrodes. Therefore, these results show that the HIS sensor using MAA enhanced the responsivity and selectivity to HIS as MIP specifically recognized HIS compared with other chemical substances.

Thus, these potentiometric results clearly show that the HIS sensor using MAA had good responsivity to, and selectivity for, HIS as a template molecule.

Conclusion

An MIP-modified sensor for HIS with good responsivity and selectivity using MAA as a functional monomer was manufactured. Unlike sensors prepared using other functional monomers, i.e., AA, AT, and 4-VP, the HIS sensor using MAA has three-dimensional HIS-recognition cavities in the MIP and can specifically recognize HIS in the cavities. The di-cationic form of HIS strongly binds with the carboxyl group of MAA via hydrogen bonds. The responsivity and selectivity of the HIS sensor using MAA are therefore better than those of the other HIS sensors. This shows that the type of intermolecular interaction influenced the potential response of the MIP-modified potentiometric sensor. It is therefore important to elucidate the intermolecular interactions between the template molecule and functional monomer for fabrication of MIP-modified potentiometric sensors. Based on the evidence obtained in this study, suitable ratios of template molecule, functional monomer, and cross-linker for MIP preparation, and quantification of the HIS sensor are currently investigated. HIS sensor

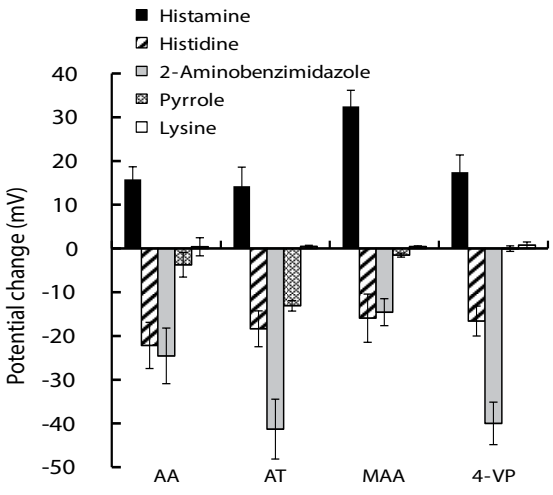

Figure 9: Selectivities of HIS sensors using each functional monomer to HIS, histidine, 2-aminobenzimidazole, pyrrole, and lysine. The determination of each HIS sensor was in triplicate.

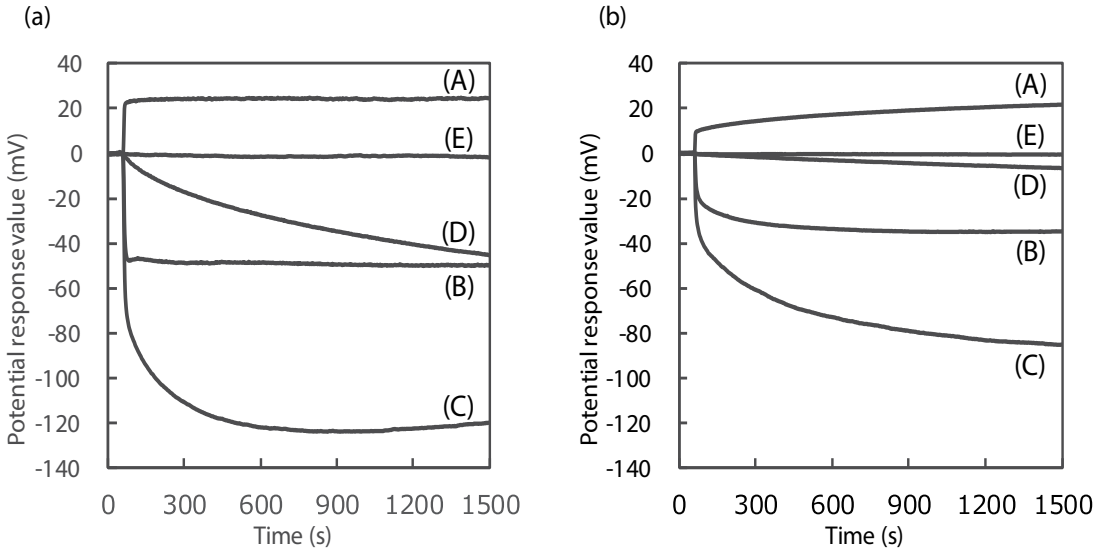

Figure 10: Potential response curves of (a) bare graphite rod electrode and (b) graphite rod electrode coated with the polymerized thin film of ethylbenzene to (A) HIS, (B) histidine, (C) 2-aminobenzimidazole, (D) pyrrole, and (E) lysine. Final concentration of chemical substances was 0.1×10^{-3} mol L^{-1}.

showed a good response to HIS concentrations of 0.1×10^{-3} mol L^{-1} and has sufficient capability to sense HIS when compared with other HIS sensors previously reported.

Acknowledgements

This work was partly supported by JSPS KAKENHI (Grant Number 21590048) for Scientific Research (C).

References

1. Iyer R, Pavlov V, Katakis I, Bachas LG (2003) Amperometric sensing at high temperature with a "wired" thermostable glucose-6-phosphate dehydrogenase from aquifex aeolicus. Anal Chem 75: 3898-3901.
2. Tani Y, Tanaka K, Yabutani T, Mishima Y, Sakuraba H, et al. (2008) Development of a $_{D}$-amino acids electrochemical sensor based on immobilization of thermostable $_{D}$-Proline dehydrogenase within agar gel membrane. Anal Chim Acta 619: 215-220.
3. Yu X, Munge B, Patel V, Jensen G, Bhirde A, et al. (2006) Carbon nanotube amplification strategies for highly sensitive immunodetection of cancer biomarkers. J Am Chem Soc 128: 11199-11205.
4. Wang X, Ioacara S, DeHennis A (2015) Long-term home study on nocturnal hypoglycemic alarms using a new fully implantable continuous glucose monitoring system in type 1 diabetes. Diabetes Technol Ther 17: 780-786.
5. Haginaka J, Sanbe H (2001) Uniformly sized molecularly imprinted polymer for (S)-naproxen retention and molecular recognition properties in aqueous mobile phase. J Chromatogr A 913: 141-146.
6. Zhang Y, Lei J (2013) Synthesis and evaluation of molecularly imprinted polymeric microspheres for chloramphenicol by aqueous suspension polymerization as a high performance liquid chromatography stationary phase. Bull Korean Chem Soc 34: 1839-1844.
7. Li H, Li D (2015) Preparation of a pipette tip-based molecularly imprinted solid-phase microextraction monolith by epitope approach and its application for determination of enkephalins in human cerebrospinal fluid. J Pharm Biomed Anal 115: 330-338.
8. Hashemi-Moghaddam H, Ahmadifard M (2016) Novel molecularly-imprinted solid-phase microextraction fibercoupled with gas chromatography for analysis of furan. Talanta 150: 148-154.
9. Svoboda P, Combes A, Petit J, Nováková L, Pichon V, et al. (2015) Synthesis of a molecularly imprinted sorbent for selective solid-phase extraction of β-N-methylamino-L-alanine. Talanta 144: 1021-1029.
10. Sreenivasan K (1999) On the application of molecularly imprinted poly(HEMA) as a template responsive release system. J Appl Polym Sci 71: 1819-1821.
11. Hiratani H, Mizutani Y, Alvarez-Lorenzo C (2005) Controlling drug release from imprinted hydrogels by modifying the characteristics of the imprinted cavities. Macromol Biosci 5: 728-733.
12. Puoci F, Iemma F, Cirillo G, Picci N, Matricardi P, et al. (2007) Molecularly imprinted polymers for 5-fluorouracil release in biological fluids. Molecules 12: 805-814.
13. Men J, Gao B, Yao L, Zhang Y (2014) Preparation and characterization of metronidazole-surface imprinted microspheres MIP-PSSS/CPVA for colon-specific drug delivery system. J Macromol Sci, Part A: Pure Appl Chem 51: 914-923.
14. Sari E, Üzek R, Duman M, Denizli A (2016) Fabrication of surface plasmon resonance nanosensor for the selective determination of erythromycin via molecular imprinted nanoparticles. Talanta 150: 607-614.
15. Florea A, Guo Z, Cristea C, Bessueille F, Vocanson F, et al. (2015) Anticancer drug detection using a highly sensitive molecularly imprinted electrochemical sensor based on an electropolymerized microporous metal organic framework. Talanta 138: 71-76.
16. Lin RY, Schwartz LB, Curry A, Pesola GR, Knight RJ, et al. (2000) Histamine and tryptase levels in patients with acute allergic reactions: An emergency department–based study. J Allergy Clin Immunol 106: 65-71.
17. Schwartz JC, Pollard H, Quach TT (1980) Histamine as a neurotransmitter in mammalian brain: neurochemical evidence. J Neurochem 35: 26-33.
18. Mahmoudi R, Norian R (2014) Occurrence of histamine in canned tuna fish from Iran. J Verbr Lebensm 9: 133-136.
19. Bao L, Sun D, Tachikawa H, Davidson V (2002) Improved sensitivity of a histamine sensor using an engineered methylamine dehydrogenase. Anal Chem 74: 1144-1148.
20. Yamada R, Fujieda N, Tsutsumi M, Tsujimura S, Shirai O, et al. (2008) Bioelectrochemical determination at histamine dehydrogenase-based electrodes. Electrochemistry 76: 600-602.
21. Veseli A, Vasjari M, Arbneshi T, Hajrizi A, Švorc Ľ, et al. (2016) Electrochemical determination of histamine in fish sauce using heterogeneous carbon electrodes modified with rhenium(IV) oxide. Sens Actuators B 228: 774-781.
22. Fukuda M, Hayashi H, Hasegawa T, Morii T (2009) Development of a fluorescent ribonucleopeptide sensor for histamine. Trans Mater Res Soc Jpn 34: 525-527.
23. Kitade T, Kitamura K, Konishi T, Takegami S, Okuno T, et al. (2004)

Potentiometric immunosensor using artificial antibody based on molecularly imprinted polymers. Anal Chem 76: 6802-6807.

24. Sun N, Avdeef A (2011) Biorelevant pK_a (37°C) predicted from the 2D structure of the molecule and its pK_a at 25°C. J Pharm Biome Anal 56: 173-182.

25. Baba T, Matsui T, Kamiya K, Nakano M, Shigeta Y (2014) A density functional study on the pK_a of small polyprotic molecules. Int J Quantum Chem 114: 1128-1134.

26. Calculated using Advanced Chemistry Development (ACD/Labs) Software V11.02

27. Piletska EV, Guerreiro AR, Romero-Guerra M, Chianella I, Turner APF, et al. (2008) Design of molecular imprinted polymers compatible with aqueous environment. Anal Chim Acta 607: 54-60.

28. Dai Z, Liu J, Tang S, Wang Y, Wang Y, et al. (2015) Optimization of enrofloxacin-imprinted polymers by computer-aided design. J Mol Model 21: 290.

29. Dong W, Yan M, Liu Z, Wu G, Li Y (2007) Effects of solvents on the adsorption selectivity of molecularly imprinted polymers; Molecular simulation and experimental validation. Sep Purif Technol 53: 183-188.

30. Shi X, Wu A, Qu G, Li R, Zhang D (2007) Development and characterization of molecularly imprinted polymers based on methacrylic acid for selective recognition of drugs. Biomaterials 28: 3741-3749.

31. Trikka FA, Yoshimatsu K, Ye L, Kyriakidis DA (2012) Molecularly imprinted polymers for histamine recognition in aqueous environment. Amino Acids 43: 2113-2124.

32. Itahara T (1998) NMR study of stacking interactions between adenine and xanthine rings. J Chem Soc, Perkin Trans 2: 1455-1462.

33. Kamiichi K, Doi M, Nabae M, Ishida T, Inoue M (1987) Structural studies of the interaction between indole derivatives and biologically important aromatic compounds. Part 19. Effect of base methylation on the ring-stacking interaction between tryptophan and guanine derivatives: a nuclear magnetic resonance investigation. J Chem Soc, Perkin Trans 2: 1739-1745.

34. Tarui M, Nomoto N, Hasegawa Y, Minoura K, Doi M, et al. (1996) Thermodynamic effect of complementary hydrogen bond base pairing on aromatic stacking interaction in the guanine-X-Trp complex (X=adenine, guanine, cytosine, thymine). Chem Pharm Bull 44: 1998-2002.

35. Perrin D, Dempsey B, Serjeant EP (1981) pKa Prediction for organic acids and bases. Chapman and Hall 107.

36. Charton M, Roche E (1977) Design of biopharmaceutical properties through prodrugs and analogs. Am Pharm Assoc Ch 9: 269.

37. Kabachnik MI, Mastryukova TA (1984) A σρ-analysis of carbon acidity of organophosphorus compounds. Zh Obshch Khim 54: 2161-2169.

38. Hansch C, Leo A, Taft RW (1991) A survey of hammett substituent constants and resonance and field parameters. Chem Rev 91: 165-195.